Controllable electron transport on the surface of a topological insulator

Jian-Hui Yuan,* Ze Cheng, Jian-Jun Zhang, Qi-Jun Zeng, and Jun-Pei Zhang

School of Physics, Huazhong University of Science and Technology, Wuhan 430074, China

(Dated: March 2, 2013)

Abstract

We theoretically study the electron transport properties in a ferromagnetic/normal/ferromagnetic tunnel junction, which is deposited on the top of a topological surface. The conductance at the parallel (**P**) configuration can be much bigger than that at the antiparallel (**AP**) configuration. Compared **P** with **AP** configuration, there exists a shift of phase which can be tuned by gate voltage. We find that the exchange field weakly affects the conductance of carriers for **P** configuration but can dramatically suppress the conductance of carriers for **AP** configuration. This controllable electron transport implies anomalous magnetoresistance in this topological spin valve, which may contribute to the development of spintronics . In addition, we find that there is a Fabry-Perot-like electron interference.

I. INTRODUCTION

The concept of a topological insulator (**TI**) dates back to the work of Kane and Mele, who focused on two-dimensional (**2D**) systems [1]. There has been much recent interest in **TIs**, three-dimensional insulators with metallic surface states protected by time reversal invariance $[1 - 25]$. Its theoretical [2] and experimental [3] discovery has accordingly generated a great deal of excitement in the condensed matter physics community. In particular, the surface of a three-dimensional (**3D**) **TI**, such as Bi_2Se_3 or Bi_2Te_3 [4], is a 2D metal, whose band structure consists of an odd number of Dirac cones, centered at time reversal invariant momenta in the surface Brillouin zone [5]. This corresponds to the infinite mass Rashba model [6], where only one of the spin-split bands exists. This has been beautifully demonstrated by the spin- and angle-resolved photoemission spectroscopy $[7, 8]$. Surface sensitive experiments such as angle-resolved photoemission spectroscopy (**ARPES**) and scanning tunneling microscopy (**STM**) $[9, 10]$ have confirmed the existence of this exotic surface metal, in its simplest form, which takes a single Dirac dispersion. Recent theoretical and experimental discovery of the two dimensional (**2D**) quantum spin Hall system $[11 - 18]$ and its generalization to the **TI** in three dimensions $[19 - 21]$ have established the state of matter in the time-reversal symmetric systems.

The time-reversal invariant **TI** is a new state of matter, distinguished from a regular band insulator by a nontrivial topological invariant, which characterizes its band structure [11]. Currently, most works focus on searching for TI materials and novel transport properties. To my knowledge, the fabrication of such TI-based nanostructure is still a challenging task. Usually such structures are fabricated by utilizing the split gate and etching technique [22]. On the other hand, the **3D TIs** are expected to show several unique properties when the time reversal symmetry is broken $[23 - 25]$. This can be realized directly by a ferromagnetic insulating (**FI**) layer attached to the **3D TI** surface. One remarkable feature of the Dirac fermions is that the Zeeman field acts like a vector potential: the Dirac Hamiltonian is transformed as $\sigma \cdot \mathbf{k} \longrightarrow \sigma \cdot (\mathbf{k} + \mathbf{H})$ by the Zeeman field $\mathbf{H}$ [26]. This is in contrast to the Schr*ö*dinger electrons in conventional semiconductor heterostructures modulated by nanomagnets $[27 - 29]$.

In this paper, we study the electron transport properties in a ferromagnetic (**F**)/normal/**N**/ ferromagnetic (**F**) tunnel junction, which is deposited on the top of a topological surface. Ferromag-

netic Permalloy electrodes are formed by electron-beam lithography (EBL) followed by thermal evaporation; a second EBL step establishes contact to the Permalloy via Cr /Au electrodes [30]. As shown in Fig.1, the **FI** is put on the top of the **TI** to induce an exchange field via the magnetic proximity effect. The easy axis of a **FI** stripe is usually along its length direction and thus either in parallel (**P**) or antiparallel (**AP**) with the $+y$ axis. We find that the conductance at the **P** configuration can be much bigger than that at the **AP** configuration. Compared **P** with **AP** configuration, there exists a shift of phase which can be tuned by gate voltage. We find that the exchange field weakly affects the conductance of carriers for **P** configuration but can dramatically suppress the conductance of carriers for **AP** configuration. This controllable electron transport implies anomalous magnetoresistance in this topological spin valve, which may contribute to the development of spintronics. In Sec. II , we introduce the model and method for our calculation. In Sec. III, the numerical analysis to our important issues is reported. Finally, a brief summary is given in sec. IV.

II.   MODEL AND METHOD

Now, let us consider a **F/N/ F** tunnel junction which is deposited on the top of a topological surface where a gate electrode is attached to the ferromagnetic material. The ferromagnetism is induced due to the proximity effect by the ferromagnetic insulators deposited on the top as shown in Fig. 1. We assume that the initial magnetization of **FI** stripes in the region I is aligned with the +y axis. In an actual experiment, one can use a magnet with very strong (soft) easy axis anisotropy to control the ferromagnetic material. Thus we focus on charge transport at the Fermi level of the surface of **TIs**, which is described by the 2D Dirac Hamiltonian

$$H = \upsilon_F \sigma \cdot \mathbf{p} + \sigma \cdot \mathbf{M} + V(x), \tag{1}$$

where σ is Pauli matrices , $\mathbf{M} = M_y(x) = M_0(\Theta(-x) + \gamma\Theta(x-L))$ is the effective exchange field and $V(x) = U_g\Theta(x)\Theta(L-x) + V_g\Theta(x-L)$ is the gate voltage, where $\gamma = +1 (-1)$ corresponds to the **P** (**AP**) configurations of magnetization and $\Theta(x)$ is the Heaviside step function.

Because of the translational invariance of the system along y direction, the equation $H\Psi(x,y) = E\Psi(x,y)$ admits solutions of the form $\Psi(x,y) = (\Psi_1(x), \Psi_2(x))^T \exp(ik_y y)$. We set $\hbar = \upsilon_F = 1$ in the following. Then, with the above Hamiltonian, the wave function in the whole system is given
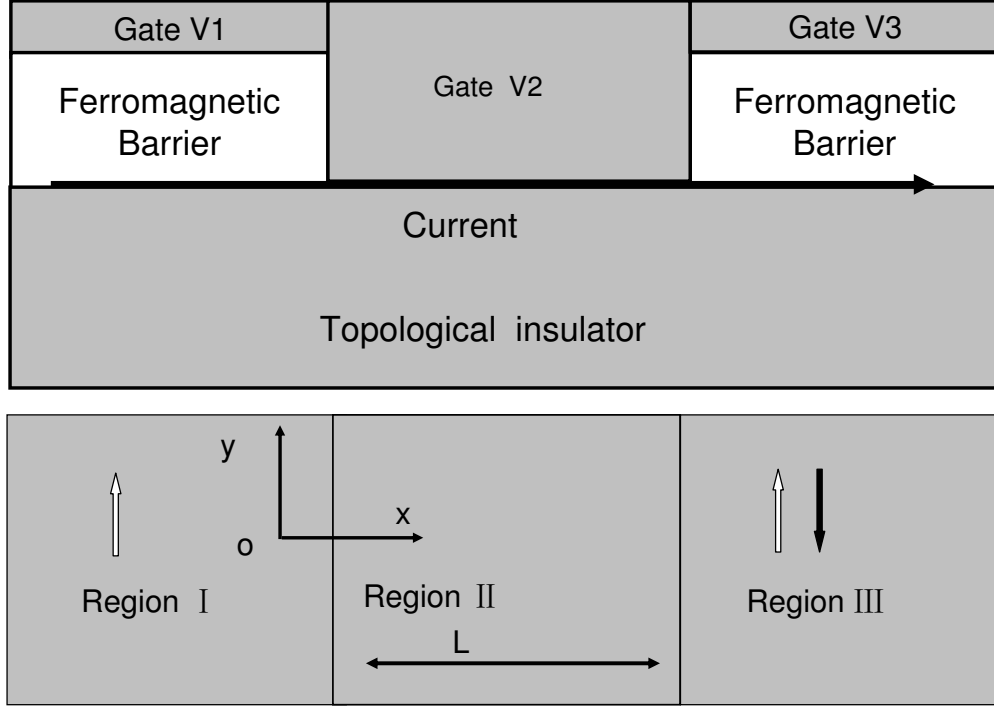
FIG. 1: Schematic illustration of the device. Top: Schematic diagram of two ferromagnetic barriers on the topological surface divided by a gate electrode at a distance L. Bottom: The magnetization directions of adjacent **FI** stripes are parallel (**P**) in the configuration and antiparallel (**AP**) in the configuration.

by

$$
\Psi_1 = \begin{cases}
\exp(ik_{x_1}x) + r\exp(-ik_{x_1}x), & x < 0, \\
\\
a\exp(iq_x x) + b\exp(-iq_x x), & 0 < x < L, \\
\\
t\exp(ik_{x_2}(x-L)), & x > L,
\end{cases}
\tag{2}
$$

$$\Psi_2 = \begin{cases} \alpha^+ \exp(ik_{x_1}x) + r\alpha^- \exp(-ik_{x_1}x), & x < 0, \\\\ a\beta^+ \exp(iq_xx) + b\beta^- \exp(-iq_xx), & 0 < x < L, \\\\ t\alpha \exp(ik_{x_2}(x-L)), & x > L, \end{cases} \tag{3}$$

where $k_{x_1} = E\cos\theta_{F_1}$, $q_x = (E-U_g)\cos\theta$ and $k_{x_2} = (E-V_g)\cos\theta_{F_2}$ are wave vectors in region I, region II and region III, $\alpha^\pm = \pm\exp(\pm i\theta_{F_1})$, $\beta^\pm = \pm\exp(\pm i\theta)$ and $\alpha = \exp(i\theta_{F_2})$. The momentum k_y conservation should be satisfied everywhere such as $k_y = E\sin\theta_{F_1} - M_0 = (E-U_g)\sin\theta = (E-V_g)\sin\theta_{F_2} - \gamma M_0$. Also, r and t are reflection and transmission coefficients, respectively. Continuities of the wave function Ψ at $x=0$ and $x=L$ are $\Psi(0^-) = \Psi(0^+)$ and $\Psi(L^-) = \Psi(L^+)$, respectively. We find that the transmitted electron coefficient t_γ is given by

$$t_\gamma = \frac{2\cos\theta_{F_1}\cos\theta\exp(-ik_{x_2}L)}{s_{1,\gamma}\cos(q_xL) + is_{2,\gamma}\sin(q_xL)}, \tag{4}$$

with $s_{1,\gamma} = \cos\theta(\exp(i\theta_{F_2}) + \exp(-i\theta_{F_1}))$ and $s_{2,\gamma} = i\sin\theta(\exp(-i\theta_{F_1}) - \exp(i\theta_{F_2})) - \exp(i(\theta_{F_2} - \theta_{F_1})) - 1$. Then

$$T_\gamma = |t_\gamma|^2\mathfrak{R}(\cos\theta_{F_2}/\cos\theta_{F_1}), \tag{5}$$

where the factor $\mathfrak{R}(\cos\theta_{F_2}/\cos\theta_{F_1})$ is due to current conservation. In the linear transport regime and for low temperature, we can obtain the conductance G by introducing it as the electron flow averaged over half the Fermi surface from the well-known Landauer-Buttiker formula [25, 31, 32]

$$G_\gamma \sim 1/2 \int_{-\pi/2}^{\pi/2} T_\gamma(E_F, E_F\cos\theta_{F_1})\cos\theta_{F_1}d\theta_{F_1}. \tag{6}$$

III. RESULTS AND DISCUSSIONS

For convenience we express all quantities in dimensionless units by means of the length of the basic unit L and the energy $E_0 = \hbar v_F/L$. For a typical value of $L = 50$ nm and the Bi_2Se_3 material $v_F = 5\times10^5$ m/s, one has $E_0 = 6.6$ meV. We set the energy of electron $E = E_F$ and also define the value η with the form $\eta = M_0/E_F$ in our calculation.
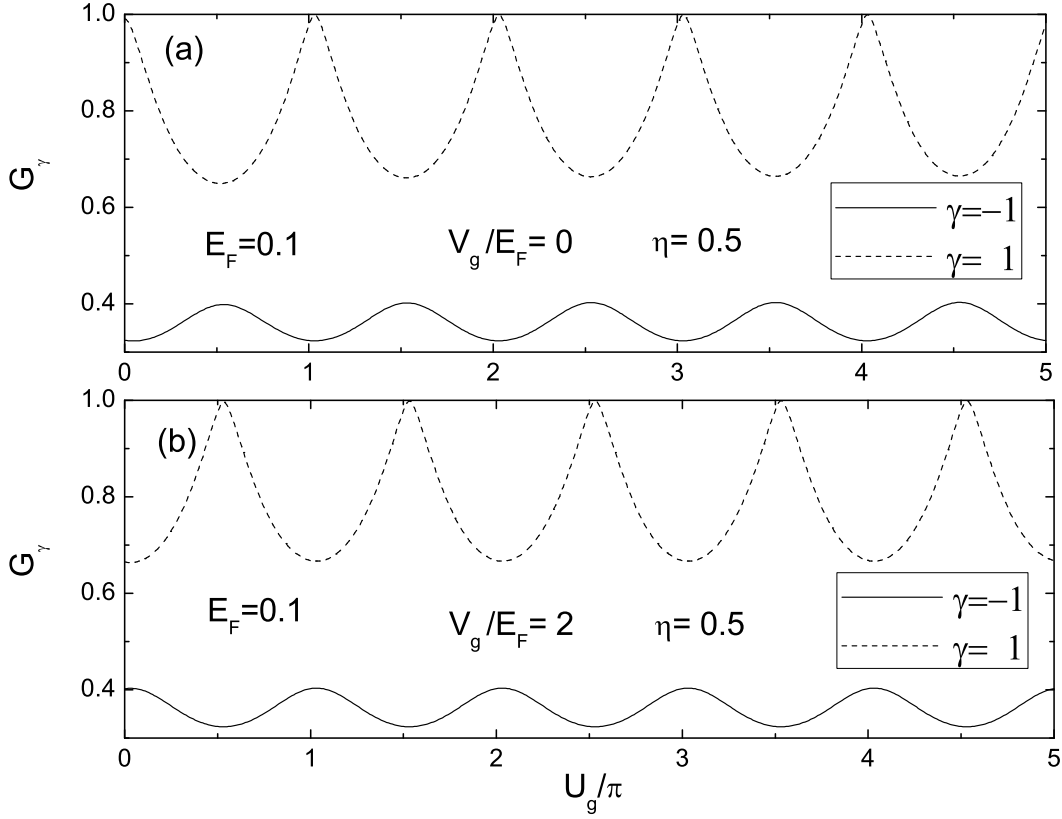
FIG. 2: Gate voltage dependence of the conductances with a **P** ($\gamma = 1$) and **AP** ($\gamma = -1$) configuration in the two cases: (a) $V_g/E_F = 0$ and (b) $V_g/E_F = 2$. The values of the other parameters are $E_F = 0.1$ and $\eta = 0.5$

In Fig.2, we show gate voltage dependence of the conductances with a **P** ($\gamma = 1$) and **AP** ($\gamma = -1$) configuration in the two cases: (a) $V_g/E_F = 0$ and (b) $V_g/E_F = 2$. The value of the other parameter is $E_F = 0.1$ and $\eta = 0.5$. The presence of quantum modulation are seen in these two figures. We can see an oscillation of the electrical conductance with a period of π when the voltage U_g is larger than E_F. The conductance at the **P** configuration can be much bigger than that at the **AP** configuration. We find that a minimum of conductance at the **P** configuration corresponds to a maximum of conductance at the **AP** configuration [see in fig.2 (a)] when the voltage U_g is larger than E_F. In Fig. 2(b), a similar tendency to Fig. 2(a) is seen. In distinct contrast to Fig.2(a), a minimum of conductance at the **P** configuration here corresponds to a maximum of conductance

6

at the **AP** configuration [see in fig.2 (b)]. That is to say, there exists a shift of π-phase. To understand these results intuitively, we consider that the gate voltage U_g is larger than the Fermi energy E_F. For the given Fermi energy $E_F = 0.1$, the condition $U_g \gg E_F$ is easily satisfied. In this limit we have $\theta \to 0$ and hence the transmission probability $T_\gamma \sim (2\cos^2\theta_{F_1}/(1 + \cos\theta_{F_1}\cos\theta_{F_2} - \cos(2U_gL)\sin\theta_{F_1}\sin\theta_{F_2})\Re(\cos\theta_{F_2}/\cos\theta_{F_1})$. For $\gamma = 1$ and $V_g/E_F = 0$ (or 2), we find the $\theta_{F_1} \equiv \theta_{F_2}$ (or $-\theta_{F_2}$), and thus $T_\gamma \sim \cos^2\theta_{F_1}/(1 - \cos^2(U_gL + \delta)\sin^2\theta_{F_1})$ where $\delta = 0$ (or $\pi/2$) corresponds to $V_g/E_F = 0$ (or 2). Thus the phase difference between $V_g/E_F = 0$ and $V_g/E_F = 2$ is given by U_gL. We find $G_\gamma \propto \cos^2(U_gL)$ for $V_g/E_F = 0$ but $G_\gamma \propto \sin^2(U_gL)$ for $V_g/E_F = 2$. When U_gL is equal to the half period of π, a minimum of conductance will appear for $V_g/E_F = 0$ but a maximum of conductance will appear for $V_g/E_F = 2$. When U_gL is equal to the period of π, a maximum of conductance will appear for $V_g/E_F = 0$ but a minimum of conductance will appear for $V_g/E_F = 2$. Furthermore, we find that G_γ oscillates between $2/3$ and 1 for $\gamma = 1$. For $\gamma = -1$ and $V_g/E_F = 0$ (or 2), there is a similar tendency to the case of $\gamma = 1$. We can see that G_γ is suppressed obviously by the strength of the effective exchange field . Nevertheless, there exists a shift of π-phase because of the factor $\cos(2U_gL)$.

In order to observe the effect of the exchange field η on the conductance, in Fig.3 we show the gate voltage dependence of the conductances with a **P** ($\gamma = 1$) and **AP** ($\gamma = -1$) configuration for four different values $\eta = 0, 0.2, 0.5$, and 0.8. The solid lines are for $V_g/E_F = 0$ while the dashed lines are for $V_g/E_F = 2$. The value of the other parameter is $E_F = 0.1$. A similar tendency to Fig. 2 is seen in Fig. 3. It is easily seen that the exchange field η weakly affects the conductance of carriers for $\gamma = 1$ but profoundly influences the conductance of carriers for $\gamma = -1$. For $\gamma = -1$, G_γ is suppressed obviously by increasing the value η. Due to current conservation, the factor $\Re(\cos\theta_{F_2}/\cos\theta_{F_1})$ must be real and then we have $\sin\theta_{F_1} = \pm\sin\theta_{F_2} + 2\eta$ where sign + (or -) corresponds to $V_g/E_F = 0$ (or 2). We can see $2\eta - 1 \leq \sin\theta_{F_1} \leq 1$ and $2\eta - 1 \leq \sin(\mp\theta_{F_2}) \leq 1$ where sign - (or +) corresponds to $V_g/E_F = 0$ (or 2). Thus we find the ranges of the angle-allowable θ_{F_1} and θ_{F_2} depend on η. The transmission is nonzero only for θ_{F_1} and θ_{F_2} in these ranges and vanishes for $\eta \geq 1$. The number of channels decreases with increasing of η, so we can see that G_γ dramatically decreases with the increase of η for $\gamma = -1$. Noting that the $\eta \geq 1$ for $\gamma = -1$, the conductance of carriers is forbidden, which implies anomalous magnetoresistance in this topological spin valve.
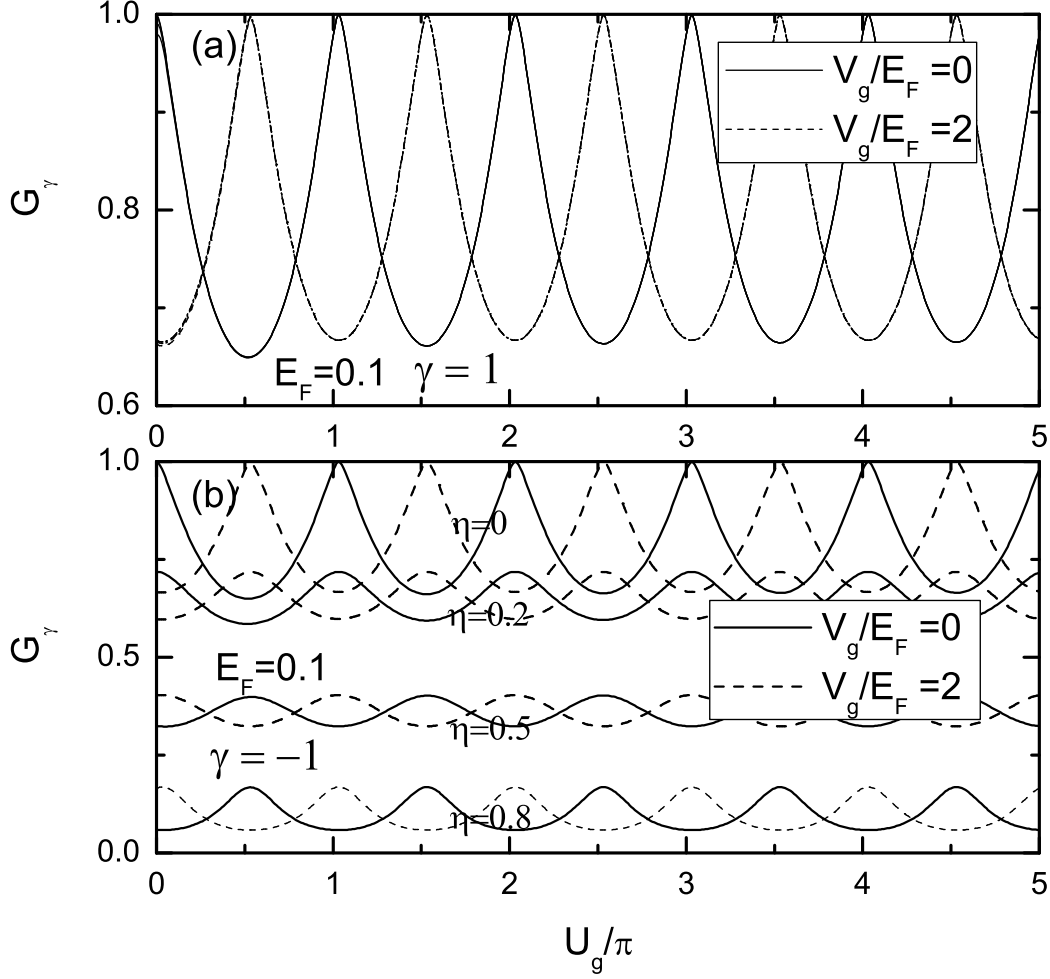
FIG. 3: Gate voltage dependence of the conductances with a **P** ($\gamma = 1$) and **AP** ($\gamma = -1$) configuration for four different values $\eta = 0, 0.2, 0.5$, and 0.8. The solid lines are for $V_g/E_F = 0$ while the dashed lines are for $V_g/E_F = 2$. The value of the other parameter is $E_F = 0.1$.

In Fig. 4, we show the gate voltage dependence of the conductances with a **P** ($\gamma = 1$) and **AP** ($\gamma = -1$) configuration for three different values $E_F = 0.1, 1.0$, and 5.0. In (a) and (b), the V_g is set as $V_g/E_F = 0$ while in (c) and (d) the V_g is set as $V_g/E_F = 2$. The value of the other parameter is $\eta = 0.5$. For $E_F = 0.1$, we can see that the π periodicity appears. However, the π periodicity is broken for $E_F = 1$ (or 5) because the condition $U_g \gg E_F$ is not satisfied for the smaller U_g. Nevertheless, we get the π periodicity of conductance again by choosing a bigger U_g
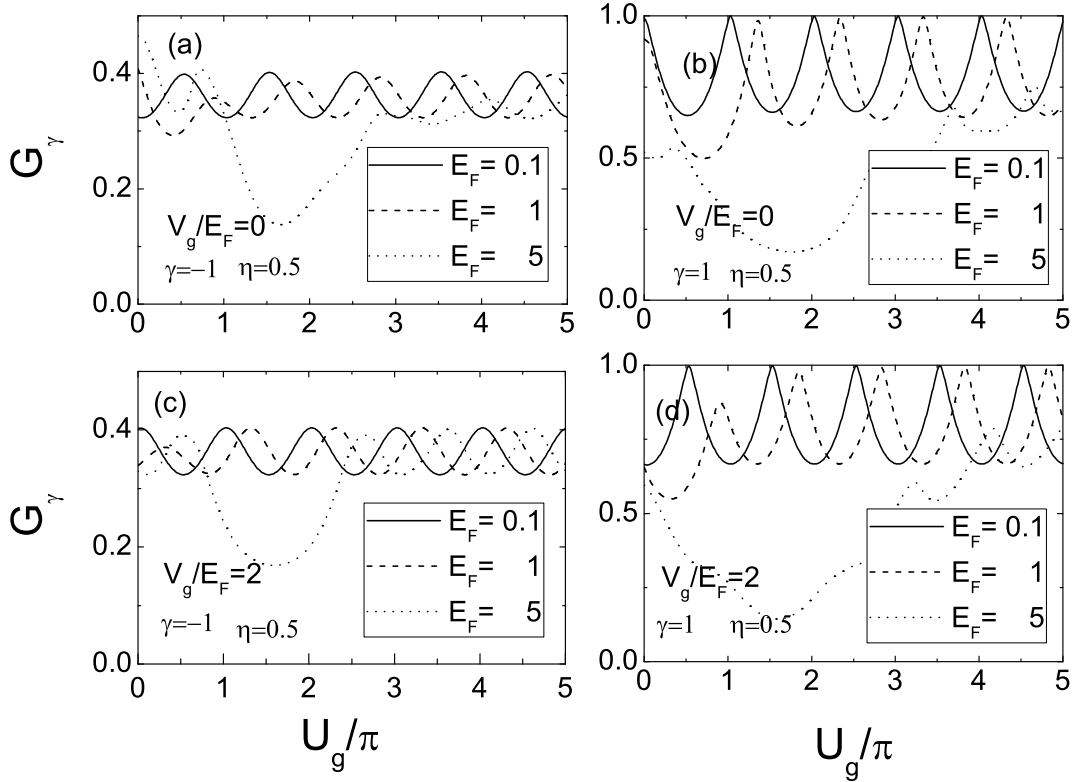
FIG. 4: Gate voltage dependence of the conductances with a **P** ($\gamma = 1$) and **AP** ($\gamma = -1$) configuration for three different values $E_F = 0.1, 1.0$, and 5.0. In (a) and (b), the V_g is set as $V_g/E_F = 0$ while in (c) and (d) the V_g is set as $V_g/E_F = 2$. The value of the other parameter is $\eta = 0.5$.

for the bigger E_F. Furthermore, we find that the minimum of the conductance will appear when the gate voltage arrives at a certain value. It is easily seen that the minimum of the conductance shifts to the right with increasing of the Fermi energy. The larger the Fermi energy is, the smaller the minimum of the conductance is. This phenomena is very obvious for the **P** ($\gamma = 1$) configuration [see in figs.4 (a) and (d)]. From Figs.4 and 5, we find that the conductance at the parallel (P) configuration can be much bigger than that at the antiparallel (AP) configuration. However it may be not satisfied for the larger Fermi energy when the gate voltage is not bigger enough. We find that there is a Fabry-Perot-like electron interference in the **F/N/F** tunnel junction, which is deposited on the top of a topological surface. The two ferromagnetic electrodes and the barrier can compose a

Fabry-Perot resonator [33, 34]. The transmitted electron waves in this resonator can be reflected by the two ferromagnetic electrodes. The electron waves undergo multiple reflections back and forth along the resonator between the two ferromagnetic electrodes. The conductance oscillations are caused by the interference of electron waves among the modes of the channel-allowable. When the gate voltage U_g is larger than the Fermi energy E_F, the round trip between the two ferromagnetic electrodes adds a further phase change $\delta \sim 4\pi/\lambda$ where the Fermi wavelength $\lambda \sim 2\pi/U_g$ because of the value $\theta \sim 0$. When the round trip between the two ferromagnetic electrodes is equal to the a multiple of wavelength, the quantum interference happens. This implies that the oscillation period is equal to $\triangle U_g = \pi$.

IV. CONCLUSION

In summary, we have theoretically investigated transport features of Dirac electrons on the surface of a three-dimensional **TI** under the modulation of a exchange field provided by an **FI** stripes. We find that the conductance at the **P** configuration can be much bigger than that at the **AP** configuration. Compared **P** with **AP** configuration, there exists a shift of phase which can be tuned by gate voltage. We find that the exchange field weakly affects the conductance of carriers for **P** configuration but can dramatically suppress the conductance of carriers for **AP** configuration. This controllable electron transport implies anomalous magnetoresistance in this topological spin valve, which may contribute to the development of spintronics .

[*] The corresponding author, E-mail: jianhui831110@163.com

[1] C. L. Kane and E. J. Mele, Phys. Rev. Lett. **95**, 146802 2005

[2] L. Fu, C. L. Kane, and E. J. Mele, Phys. Rev. Lett. **98**, 106803 (2007).

[3] D. Hsieh, D. Qian, L. Wray, Y. Xia, Y. Hor, R. J. Cava, and M. Z. Hasan, Nature (London) **452**, 970 (2008).
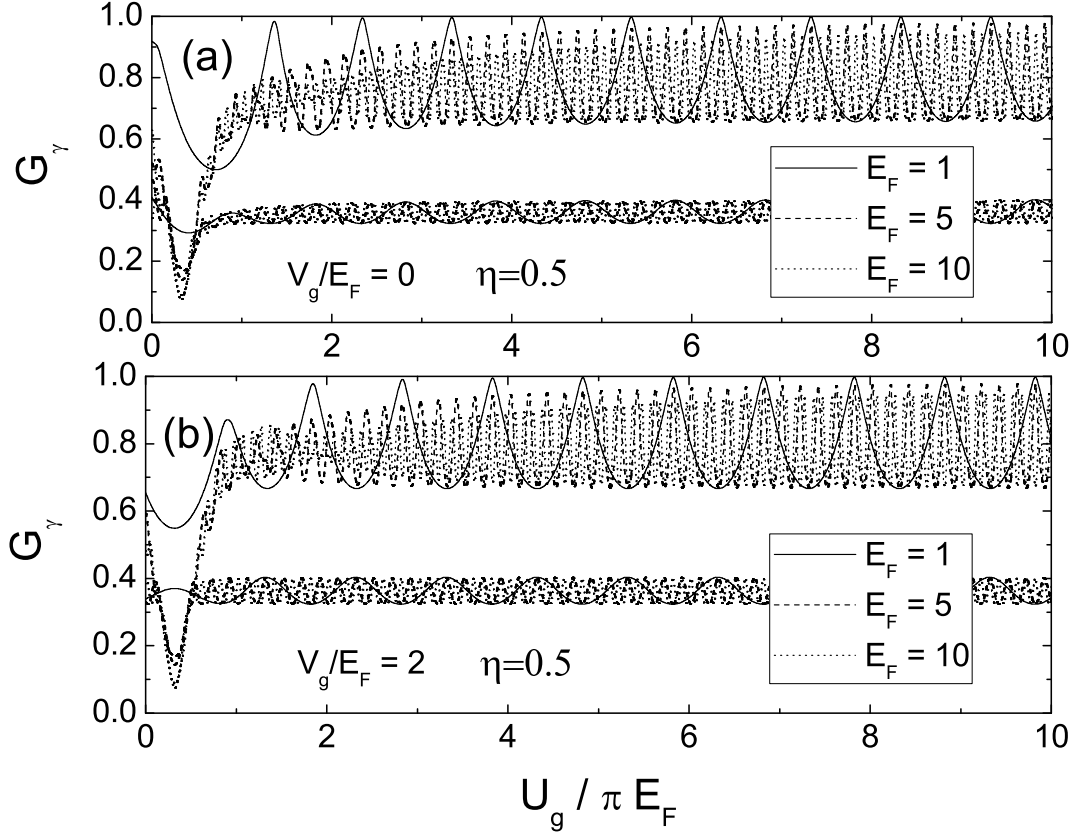
FIG. 5: Gate voltage dependence of the conductances with a **P** ($\gamma = 1$) and **AP** ($\gamma = -1$) configuration for three different values $E_F = 1.0, 5.0$, and 10.0. In (a) , the V_g is set as $V_g/E_F = 0$ while in (b) V_g is set as $V_g/E_F = 2$. The value of the other parameter is $\eta = 0.5$.

[4] Y. Xia, D. Qian, D. Hsieh, L. Wray, A. Pal, H. Lin, A. Bansi, D. Grauer, Y. S. Hor, R. J. Cava , M. Z. Hasan, Nature Phys. **5**, 398 (2009)

[5] T. Eguchi, P. Gilkey, and A. Hansen, Phys. Rep. **66**, 213 (1980)

[6] E. I. Rashba, Sov. Phys. Solid State **2**, 1109 (1960)

[7] D. Hsieh, Y. Xia, L. Wray, D. Qian, A. Pal, J. H. Dil, J. Osterwalder, F. Meier, G. Bihlmayer, C. L. Kane, Y. S. Hor, R. J. Cava, and M. Z. Hasan, Science **323**, 919 (2009)

[8] A. Nishide, A. Taskin, Y. Takeichi, T. Okuda, A. A. Kakizaki, T. Hirahara, K. Nakatsuji, F. Komori, Y. Ando, and I. Matsuda, Phys. Rev. B **81**, 041309 (2010)

[9] X.-L. Qi and S.-C. Zhang, Phys. Today **63**, 33 (2010)

[10] M. Z. Hasan and C. L. Kane, Rev. Mod. Phys. **82**, 3045 (2010).

[11] M. Z. Hasan and C. L. Kane, Rev. Mod. Phys. **82**, 3045 (2010)

[12] B. A. Bernevig and S. C. Zhang, Phys. Rev. Lett. **96**, 106802 2006

[13] C. Wu, B. A. Bernevig, and S. C. Zhang, Phys. Rev. Lett. **96**, 106401 2006

[14] C. Xu and J. E. Moore, Phys. Rev. B **73**, 045322 2006

[15] L. Fu and C. L. Kane, Phys. Rev. B **74**, 195312 (2006)

[16] X.-L. Qi, T. L. Hughes, and S.-C. Zhang, Phys. Rev. B **78**, 195424 (2008)

[17] B. A. Bernevig, T. L. Hughes, and S. C. Zhang, Science **314**, 1757 (2006)

[18] M. König, S. Wiedmann, C. Brüne, A. Roth, H. Buhmann, L. Molenkamp, X.-L. Qi, and S.-C. Zhang, Science **318**, 766 (2007)

[19] J. E. Moore and L. Balents, Phys. Rev. B **75**, 121306(R) (2007)

[20] L. Fu, C. L. Kane, and E. J. Mele, Phys. Rev. Lett. **98**, 106803 (2007)

[21] J. C. Y. Teo, L. Fu, and C. L. Kane, Phys. Rev. B **78**, 045426 (2008)

[22] Chang K and Lou W K, Phys. Rev. Lett. **106** 206802 (2011)

[23] Q. Liu, C. X. Liu, C. Xu, X. L. Qi, and S. C. Zhang, Phys. Rev. Lett. **102**, 156603 (2009)

[24] X. L. Qi, R. D. Li, J. D. Zang, and S. C. Zhang, Science **323**, 1184 (2009)

[25] X. L. Qi, T. L. Hughes, and S. C. Zhang, Phys. Rev. B **78**, 195424 (2008)

[26] T. Yokoyama, Y. Tanaka, and N. Nagaosa, Phys. Rev. B **81**, 121401(R) (2010);

[27] S. J. Lee, S. Souma, G. Ihm, and K. J. Chang, Phys. Rep. **394**, 1 (2004)

[28] M. Cerchez, S. Hugger, T. Heinzel, and N. Schulz, Phys. Rev. B **75**, 035341 (2007)

[29] A. Matulis, F. M. Peeters, and P. Vasilopoulos, Phys. Rev. Lett. **72**, 1518 (1994)

[30] Sungjae Cho, Yung-Fu Chen and Michael S. Fuhre, Appl. Phys. Lett. **91**, 123105 (2007)

[31] I. Snyman and C. W. J. Beenakker, Phys. Rev. B **75**, 045322 (2007)

[32] Ya Zhang and Feng Zhai, Appl. Phys. Lett. **96**, 172109 (2010)

[33] A. R. Akhmerov, Johan Nilsson, and C.W. J. Beenakker, Phys. Rev. Lett. **102**, 216404 (2009)

[34] P. Adroguer, C. Grenier, D. Carpentier, J. Cayssol, P. Degiovanni, and E. Orignac, Phys. Rev. B **82**, 081303(R) (2010)